

1.6 Fourier transform method

The Fourier transform (FT) method requires considerably more mathematical background than did the previous two methods. Computationally, it is the fastest known method. We will in the exercises see how we from this method mathematically can derive both the filtered back projection method and Radon's original inversion formula (which, as we noted before, is mathematically compact but numerically impractical).

1.6.1 Analytical description

We assume as before that the density of the object is represented by a density function $f(x, y)$ where x and y denote the two spatial directions. The FT method is a technique to obtain the 2-D Fourier transform

$$\hat{f}(\omega_x, \omega_y) = \frac{1}{(2\pi)^2} \int_{-\infty}^{\infty} \int_{-\infty}^{\infty} f(x, y) e^{-i\omega_x x} e^{-i\omega_y y} dx dy \quad (1.1)$$

from the scan data. The density function $f(x, y)$ can then be recovered by

$$f(x, y) = \int_{-\infty}^{\infty} \int_{-\infty}^{\infty} \hat{f}(\omega_x, \omega_y) e^{i\omega_x x} e^{i\omega_y y} d\omega_x d\omega_y \quad (1.2)$$

We will give two descriptions of how one can arrive at the FT method. The most heuristic one follows below. A more concise (but much less intuitive) is given in the exercise section.

The key step of turning the scan data into $\hat{f}(\omega_x, \omega_y)$ rests on two observations:

- Noting what happens if we send in the X-rays in a direction parallel to the x -axis:

The left part of Figure 1.1 illustrates how we obtain the scan data $g(y) = \int_{-\infty}^{\infty} f(x, y) dx$. Its 1-D Fourier transform is

$$\begin{aligned} \hat{g}(\omega_y) &= \frac{1}{2\pi} \int_{-\infty}^{\infty} g(y) e^{-i\omega_y y} dy = \frac{1}{2\pi} \int_{-\infty}^{\infty} \left[\int_{-\infty}^{\infty} f(x, y) dx \right] e^{-i\omega_y y} dy = \\ &= \frac{1}{2\pi} \int_{-\infty}^{\infty} \int_{-\infty}^{\infty} f(x, y) e^{-i0x} e^{-i\omega_y y} dx dy = 2\pi \hat{f}(0, \omega_y), \end{aligned}$$

i.e. we have obtained $\hat{f}(\omega_x, \omega_y)$ along a vertical line through origin in the (ω_x, ω_y) -plane (cf. the right part of Figure 1.1).

- Considering the difference if the X-rays would have entered from another direction.

If the X-rays had entered from an angle θ (Table 1.1 a), the collected scan data will be exactly the same as if instead, the object had been turned an angle of $-\theta$ (Table 1.1 b). As is shown in Section on Fourier transforms, turning an object turns its Fourier transform exactly the same angle. Therefore, we obtain in this case values for $\hat{f}(\omega_x, \omega_y)$ along the line through the origin in the (ω_x, ω_y) -plane orthogonal to the X-ray direction in the physical plane (Table 1.1 c,d). When we have taken X-ray images for $0 \leq \theta < \pi$ (and applied the 1-D Fourier transform to them), we have actually obtained $\hat{f}(\omega_x, \omega_y)$ along all radial lines through the origin, i.e. throughout the complete (ω_x, ω_y) -plane. The density function $f(x, y)$ is then recovered by the 2-D Fourier transform (1.2).

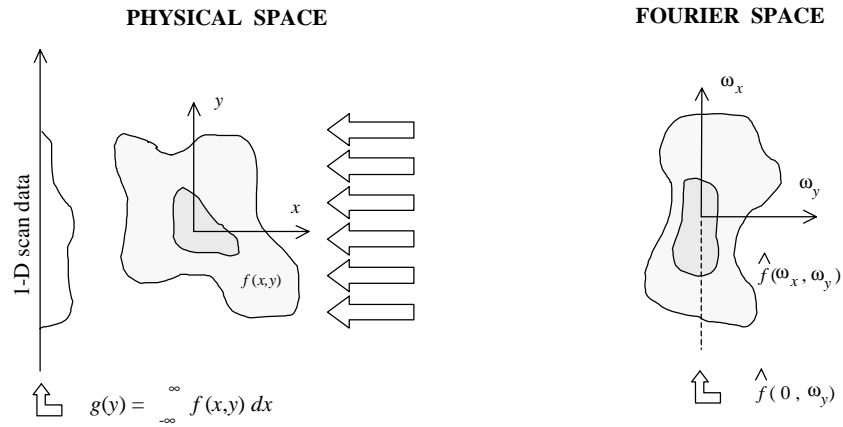


Figure 1.1: Recording with rays parallel to the x -axis, and the corresponding data set in Fourier space.

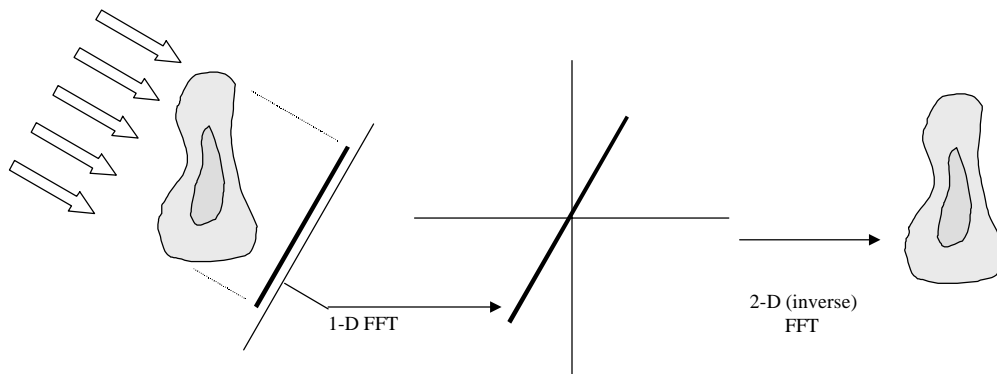
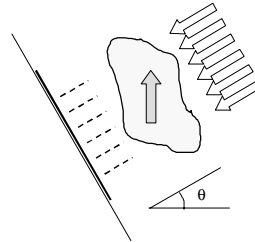
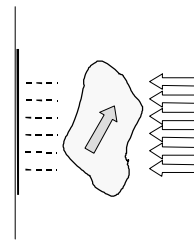


Figure 1.2: Schematic illustration of the steps in the Fourier reconstruction method.

a.
Scan with incoming X-rays at angle θ .
The density of the object is $f(x,y)$.



b.
Entirely equivalent recording as in part a:
object turned an angle θ and recording
made with X-rays entering horizontally.



c.
The 1-D Fourier transform of the recording
in part b provides a line of data along the
 ω_x -axis of a 2-D Fourier representation of
the turned object.



d.
According to the theorem stating that the
Fourier transform is rotated in the (ω_x, ω_y) -
plane the same way as a function is rotated
in the (x,y) -plane, we have now obtained
the function $\hat{f}(\omega_x, \omega_y)$ along a line through
the origin in the (ω_x, ω_y) -plane, sloping the
same way as the scan line in part a.

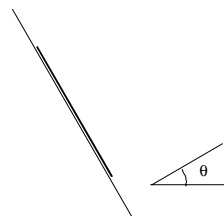


Table 1.1: Fundamental principle behind the FT method for tomographic reconstruction

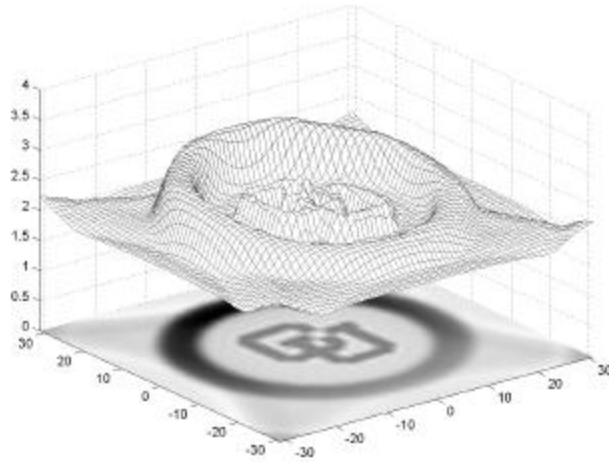


Figure 1.3: Reconstruction by direct FT method from 63 ray, 64 angle scan data to a 64×64 grid.

1.6.2 Numerical results with FT method

Following the description above gives a reconstruction as shown in Figure 1.3. Although the details in the center is near-perfect, we see a quite disturbing wobble in the base level of the reconstruction. The FT method that is implemented in the Matlab code in Section VI.1.5. contains one more refinement. Each scan vector is 'padded' to double length by just adding zeros at each end of it. Once brought to Fourier space, it is laid out on a correspondingly enlarged 2-D (ω_x, ω_y) -plane. After returning (by the inverse 2-D FFT) to the (x,y) -plane, we keep only the central square; i.e. disregard the borders (containing 3/4 of the total reconstructed area - these borders only contain an image of the padding areas). The resulting picture (produced by the code in Section VI.1.5) is seen in Figure 1.4. There are a couple of ways to understand why this padding idea helps:

- Very heuristically: We are using periodic FFTs instead of infinite-domain transforms. Periodic images of the object are then present near the boundaries of the shown domain. Discrepancies between the concept of periodicity in polar- and in Cartesian coordinates cause a difficult-to-analyze error pattern. From this loose argument, one might expect that padding would improve the image by increasing the distances to unphysical ghost images.
- More theoretically: Extending the spatial domain by a factor of two means that in each direction a twice as *dense* set of Fourier modes become available. (In a 1-D spatial domain of $[-\pi, \pi]$, modes $\dots e^{-3ix}, e^{-2ix}, e^{-ix}, e^{0ix}, e^{1ix}, e^{2ix}, e^{3ix}, \dots$ are available. If the domain is extended to $[-2\pi, 2\pi]$, also the intermediate modes $\dots e^{-\frac{5}{2}ix}, e^{-\frac{3}{2}ix}, e^{-\frac{1}{2}ix}, e^{\frac{1}{2}ix}, e^{\frac{3}{2}ix}, e^{\frac{5}{2}ix} \dots$ become present.) The interpolation from polar to Cartesian grids occurs in Fourier space. So with a denser grid in that space, interpolation becomes more accurate.

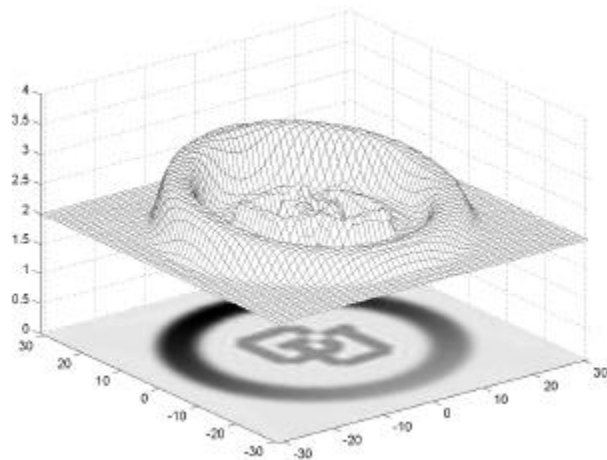


Figure 1.4: Same Fourier reconstruction as in the previous figure, but with the spatial domain 'padded' by a factor of two within the FT algorithm.

It is important to use better than-linear-interpolation (our code uses cubic interpolation). We can illustrate this in 1-D by trying to represent a half-integer mode $e^{i(n+\frac{1}{2})x}$ on a grid (in Fourier space) that only has integer modes e^{ikx} , $k=\dots-3,-2,-1,0,1,2,3,\dots$ available. Linear (second order) interpolation gives

$$e^{i(n+\frac{1}{2})x} \approx \frac{1}{2}e^{inx} + \frac{1}{2}e^{i(n+1)x} = e^{i(n+\frac{1}{2})x} \left(\frac{e^{-i\frac{1}{2}x} + e^{i\frac{1}{2}x}}{2} \right) = e^{i(n+\frac{1}{2})x} \cos \frac{x}{2}$$

and fourth order interpolation (cf. Table ...)

$$e^{i(n+\frac{1}{2})x} \approx -\frac{1}{16}e^{i(n-1)x} + \frac{9}{16}e^{inx} + \frac{9}{16}e^{i(n+1)x} - \frac{1}{16}e^{i(n+2)x} = e^{i(n+\frac{1}{2})x} \left(\frac{9}{8} \cos \frac{x}{2} - \frac{1}{8} \cos \frac{3x}{2} \right)$$

The interpolation would have been perfect, had the factors multiplying $e^{i(n+\frac{1}{2})x}$ in the RHSs in the two equations above been equal to one. Figure 1.5 displays the actual factor for interpolation of different orders (note that this factor depends on x only, i.e. not on n). Interpolation by order 4 and above achieves excellent results in the center of the domain. Hence, we can expect good reconstruction where, in the padded case, the object is located.

Although a factor two padding leads internally to a larger grid, the operation count still remains $O(n^2 \log n)$ (the proportionality constant has increased around a factor of four).

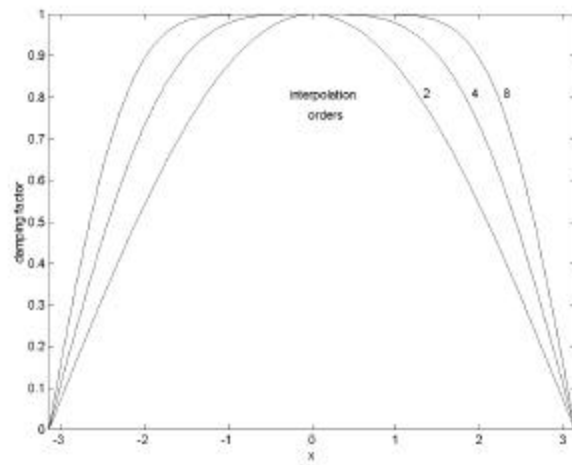


Figure 1.5: The damping factor at different physical locations across the domain when a half-integer Fourier mode is interpolated *in Fourier space* to integer frequencies.